J. Appl. Comput. Mech., 8(2) (2022) 723-732
DOI: 10.22055/JACM.2022.38968.3317

ISSN: 2383-4536
jacm.scu.ac.ir

Shahid Chamran
University of Ahvaz

Journal of
Applied and Computational Mechanics

Research Paper

Strength of Steel Shell Cylindrical Panels Reinforced with an Orthogonal Grid of Stiffeners

Alexey Semenov

Department of Computer Science, Saint Petersburg State University of Architecture and Civil Engineering, 4, 2nd Krasnoarmeyskaya st., Saint-Petersburg, 190005, Russia

Received October 22 2021; Revised December 27 2021; Accepted for publication January 02 2022.
Corresponding author: A. Semenov (sw.semenov@gmail.com)

Abstract. The paper presents an approach to the strength analysis in steel cylindrical panels reinforced from the concave side with an orthogonal grid of stiffeners. A mathematical model of the Timoshenko (Mindlin – Reissner) type is used. Transverse shears and geometric nonlinearity are taken into account. The stiffeners are introduced in two ways: using the method of refined discrete introduction (proposed by author) and the method of structural anisotropy. Computational algorithm based on the Ritz method and the best parameter continuation method. For strength analysis von Mises criterion is used. The values of the maximum permissible strength loss loads are shown for several variants of structures made of steel S345. The extension of areas of non-fulfillment of strength conditions according to the Mises criterion for the stiffened and unstiffened structures are shown.

Keywords: Cylindrical panels, Ritz method, shells, stiffeners, strength.

1. Introduction

Thin-walled structures are commonly used for solving a wide class of applied challenges, including the problems of mechanical engineering, construction building, and transport industry. Such structures, made of many different materials (from metals to composites and wood), are often used as hangars for vehicles, coverings and floors of industrial buildings, light structures in shipbuilding, aerospace and so on. At the same time, thin-walled structures often need to include stiffeners with the scope to achieve the design requirements for stiffness and resistance.

It is significantly more difficult to study stiffened structures than structures of uniform thickness considering how these geometric non-uniformities do not allow the application of theoretical approaches and simplifying models [1–3]. Thus, the need to use more complex techniques such as numerical simulations with numerical models based on experimental verifications becomes inaudible. This is detailed, e.g., in [4] where a finite element (FE) model was developed and validated with the scope to investigate the stiff and buckling behaviour of extra-large stiffened structures.

In this regard, there are several approaches to the introduction of stiffeners and for evaluating their effects on the structures. For instance, some papers (Jaunky et al. [5]; Kidane et al. [6]) distinguish two types of approaches to account for stiffeners in a structure: a discrete approach [7–11] and a stiffness smearing approach [12–15].

Sadeghifar, Bagheri and Jafari [10] investigates the influence of nonuniformity of eccentricity of stringers on the general axial buckling load of stiffened laminated cylindrical shells with simply supported end conditions. The critical loads are calculated using Love's FSDT and solved using the Rayleigh-Ritz procedure. In Tu and Loi [15] a free vibration analysis of rotating functionally graded cylindrical shells with orthogonal stiffeners are presents. Based on Love's first approximation theory and smeared stiffeners technique, the governing equations of motion which take into account the effects of initial hoop tension and also the centrifugal and Coriolis forces due to rotation are derived. Finally, in Lanzo and Garcea [16] thin-walled complex structures were investigated by the so-called Koiter's analysis.

Therefore, the need to develop consolidated methods for optimizing reinforced structures becomes evident. Referring to simple geometries, such as plates reinforced by the addition of stiffeners, there are many works available in the literature as in Pinto et al [17] where a multiobjetive approach to the geometrical optimization was develop. Optimization of stiffened cylindrical shells to solve specific practical tasks was addressed by Bai et al. [18], Chen et al. [19], Lene et al. [20], Reza Ghasemi et al. [21] and Hao et al. [22].

Wang et al. [23] presented general similitude requirements and the scaling laws for nonlinear buckling of stiffened orthotropic shallow spherical shells by applying similitude transformation to the total energy of the structural system. Cho et al. [24] reports experimental and numerical investigations on the ultimate strength responses of steel-welded, ring-stiffened conical shells when subjected to external hydrostatic pressure. The numerical computations were performed on the finite element code of ABAQUS FEA. The imperfection due to fabrication, such as initial out-of-circularity, and residual stresses due to welding are simulated. Strength problems of shell structures were considered, for example, in Duarte et al. [25], Brauns and Skadins [26], Abrosimov and Novosel'tseva [27] and Semenov [28].

Published online: January 08 2022

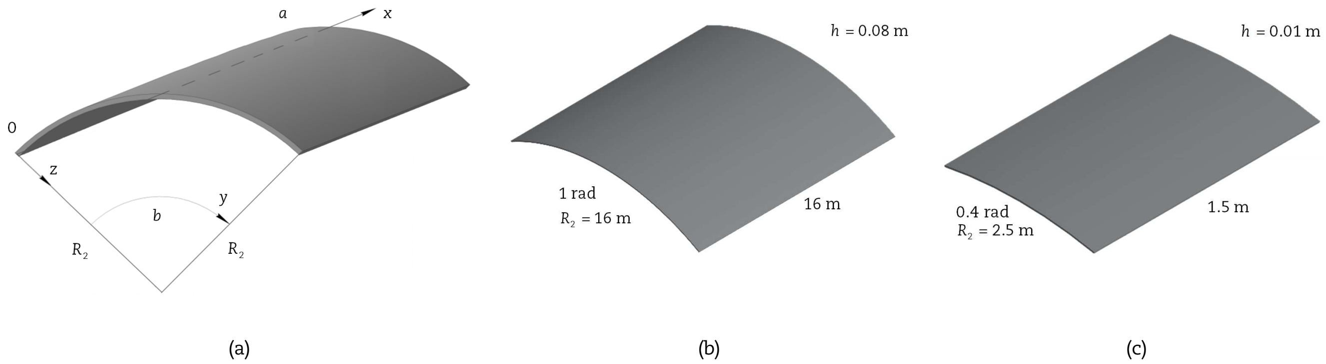

Fig. 1. Cylindrical shell panel. a) Local coordinate system; b) Option No. 1; c) Option No. 2.

In [25] a comparative study between Hashin damage criterion and the eXtended Finite Element Method (XFEM) applied to the failure of plates made of fiber reinforced polymers (FRP). A brief literature review on failure criteria is also presented in the paper and Finite element models of square plates with different layer configurations are described within the framework of ABAQUS package. A similar numerical approach was used in Pavlovic et al. [29] when FRP tridimentional plates where modelled and optimized by ANSYS in the case of very large and thin functional structures.

The purpose of this paper is to describe the methodology for analyzing the strength of cylindrical panels, stiffened by an orthogonal mesh of ribs, based on different approaches to the introduction of reinforcing elements.

2. Theory and Methods

2.1 Mathematical Model

Consider thin-walled shells under external mechanical loading. The geometry of these structures is defined by the Lame parameters A, B and radii of principal curvatures R_1, R_2 along the x, y coordinates, respectively. For cylindrical panels $A = 1, B = R_2, R_1 = \infty, R_2 = \text{const}$.

It will be used a mathematical model of the Timoshenko (Mindlin–Reissner) type, which takes into account transverse shears, material orthotropy, and geometric nonlinearity. According to this model, in the case of static problems, three functions characterizing displacement of the coordinate surface points $U(x,y), V(x,y), W(x,y)$ and two functions characterizing the normal rotation angles in the planes xOz, yOz ($\Psi_x(x,y), \Psi_y(x,y)$) will be the unknown functions. This model is based on the functional of total potential deformation energy, which can be written in the following form:

$$E_s = E_s^0 + E_p^R,$$

$$E_s^0 = \frac{1}{2}\int_{a_1}^{a}\int_{0}^{b}\Big(N_x^0\varepsilon_x + N_y^0\varepsilon_y + \frac{1}{2}\left(N_{xy}^0 + N_{yx}^0\right)\gamma_{xy} + M_x^0\chi_1 + M_y^0\chi_2 + \left(M_{xy}^0 + M_{yx}^0\right)\chi_{12} + Q_x^0\left(\Psi_x - \theta_1\right) + Q_y^0\left(\Psi_y - \theta_2\right) - 2qW - 2P_xU - 2P_yV\Big)AB\,dx\,dy, \tag{1}$$

$$E_p^R = \frac{1}{2}\int_{a_1}^{a}\int_{0}^{b}\Big(N_x^R\varepsilon_x + N_y^R\varepsilon_y + \frac{1}{2}\left(N_{xy}^R + N_{yx}^R\right)\gamma_{xy} + M_x^R\chi_1 + M_y^R\chi_2 + \left(M_{xy}^R + M_{yx}^R\right)\chi_{12} + Q_x^R\left(\Psi_x - \theta_1\right) + Q_y^R\left(\Psi_y - \theta_2\right)\Big)AB\,dx\,dy,$$

where q, P_x, P_y denote load components; N_x, N_y denote normal forces in the direction of the x,y coordinates; N_{xy}, N_{yx} denote shear forces in the corresponding plane xOy; M_x, M_y denote bending moments; M_{xy}, M_{yx} denote torque moments; Q_x, Q_y denote transverse forces in the planes xOz and yOz, which are defined by the following relationships for the structural skin (superscript 0):

$$N_x^0 = \frac{E_1 h}{1-\mu_{12}\mu_{21}}\left(\varepsilon_x + \mu_{21}\varepsilon_y\right), \quad N_y^0 = \frac{E_2 h}{1-\mu_{12}\mu_{21}}\left(\varepsilon_y + \mu_{12}\varepsilon_x\right), \quad N_{xy}^0 = N_{yx}^0 = G_{12}h\gamma_{xy},$$
$$M_x^0 = \frac{E_1 h^3}{12(1-\mu_{12}\mu_{21})}\left(\chi_1 + \mu_{21}\chi_2\right), \quad M_y^0 = \frac{E_2 h^3}{12(1-\mu_{12}\mu_{21})}\left(\chi_2 + \mu_{12}\chi_1\right), \quad M_{xy}^0 = M_{yx}^0 = \frac{G_{12}h^3}{6}\chi_{12}, \tag{2}$$
$$Q_x^0 = G_{13}kh\left(\Psi_x - \theta_1\right), \quad Q_y^0 = G_{23}kh\left(\Psi_y - \theta_2\right).$$

Here E_1, E_2 denote elasticity moduli in the directions x, y; $k = 5/6$; G_{12}, G_{13}, G_{23} denote shear moduli in the planes xOy, xOz, yOz, respectively; μ_{12}, μ_{21} denote Poisson's ratios; $\varepsilon_x, \varepsilon_y$ denote tensile strains; γ_{xy} denotes shear strains in the plane xOy; $\chi_1, \chi_2, \chi_{12}$ denote functions of change in curvature and torsion as follows:

$$\varepsilon_x = \frac{1}{A}\frac{\partial U}{\partial x} + \frac{1}{AB}V\frac{\partial A}{\partial y} - k_xW + \frac{1}{2}\theta_1^2, \quad \varepsilon_y = \frac{1}{B}\frac{\partial V}{\partial y} + \frac{1}{AB}U\frac{\partial B}{\partial x} - k_yW + \frac{1}{2}\theta_2^2, \quad \gamma_{xy} = \frac{1}{A}\frac{\partial V}{\partial x} + \frac{1}{B}\frac{\partial U}{\partial y} - \frac{1}{AB}U\frac{\partial A}{\partial y} - \frac{1}{AB}V\frac{\partial B}{\partial x} + \theta_1\theta_2,$$
$$\theta_1 = -\left(\frac{1}{A}\frac{\partial W}{\partial x} + k_xU\right), \quad \theta_2 = -\left(\frac{1}{B}\frac{\partial W}{\partial y} + k_yV\right), \quad k_x = \frac{1}{R_1}, \quad k_y = \frac{1}{R_2}, \tag{3}$$
$$\chi_1 = \frac{1}{A}\frac{\partial \Psi_x}{\partial x} + \frac{1}{AB}\frac{\partial A}{\partial y}\Psi_y, \quad \chi_2 = \frac{1}{B}\frac{\partial \Psi_y}{\partial y} + \frac{1}{AB}\frac{\partial B}{\partial x}\Psi_x, \quad \chi_{12} = \frac{1}{2}\left(\frac{1}{A}\frac{\partial \Psi_y}{\partial x} + \frac{1}{B}\frac{\partial \Psi_x}{\partial y} - \frac{1}{AB}\frac{\partial B}{\partial x}\Psi_y - \frac{1}{AB}\frac{\partial A}{\partial y}\Psi_x\right),$$

Geometric nonlinearity is taken into account in expressions for deformations (3) due to terms with variables θ. When the variables θ are multiplied, the products of the displacement functions obtained.

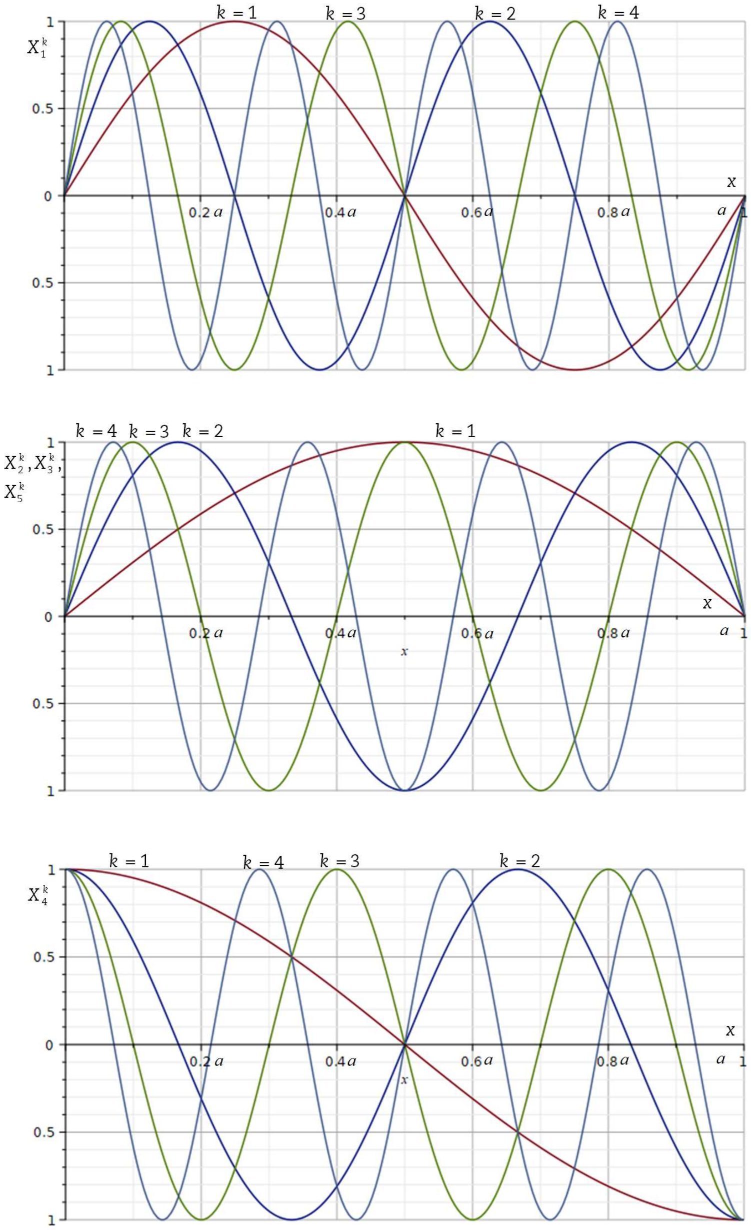

Fig. 2. Graphical representation of functions used for approximation.

On the side of the concavity, the shell is reinforced by an orthogonal mesh of stiffeners, parallel to the coordinate lines. The stiffeners are characterized by the following parameters: h^j, h^i – height of stiffeners, parallel to the axes y and x respectively; r_j, r_i – width of, respectively, j-th and i-th stiffeners; stiffeners, parallel to the axis y (j-th stiffeners) located at $a_j \le x \le b_j$, and stiffeners, parallel to the axis x (i-th stiffeners) located at $c_i \le y \le d_i$.

There are various ways to account for the presence of stiffeners. Earlier in [30], the following were considered in detail: discrete introduction of stiffeners in contact with the skin along the line (Lurie), discrete input of stiffeners in contact with the skin along the strip (Karpov), the introduction of stiffeners when “smearing” the stiffness by the method of constructive anisotropy (Karpov), as well as a new (refined) version of discrete insertion of stiffeners in contact with the skin along the strip (Semenov). Due to the cumbersomeness, all these relations here are not presents.

2.2 Algorithm for the Solution of Strength Problems

To solve a buckling analysis problem in a shell structure, to find the minimum of the functional (1) are needs. For that purpose, it’s applied the Ritz method to reduce the variational problem of finding the functional minimum to solving a system of nonlinear algebraic equations. In this case, the unknown functions can be presented in the following form:

$$U(x,y)=\sum_{k=1}^{n}\sum_{l=1}^{n}U_{kl}X_1^kY_1^l,\quad V(x,y)=\sum_{k=1}^{n}\sum_{l=1}^{n}V_{kl}X_2^kY_2^l,\quad W(x,y)=\sum_{k=1}^{n}\sum_{l=1}^{n}W_{kl}X_3^kY_3^l,\quad \Psi_x(x,y)=\sum_{k=1}^{n}\sum_{l=1}^{n}\Psi_{x_{kl}}X_4^kY_4^l,\quad \Psi_y(x,y)=\sum_{k=1}^{n}\sum_{l=1}^{n}\Psi_{y_{kl}}X_5^kY_5^l, \tag{4}$$

where $U_{kl}, V_{kl}, W_{kl}, \Psi_{x_{kl}}, \Psi_{y_{kl}}$ denote unknown numerical parameters, $X_1^k,\ldots,X_5^k$ and $Y_1^l,\ldots,Y_5^l$ denote known approximating functions with arguments x and y, satisfying the given boundary conditions. The boundary conditions for a particular structure are determined based on the type of shell contour support.

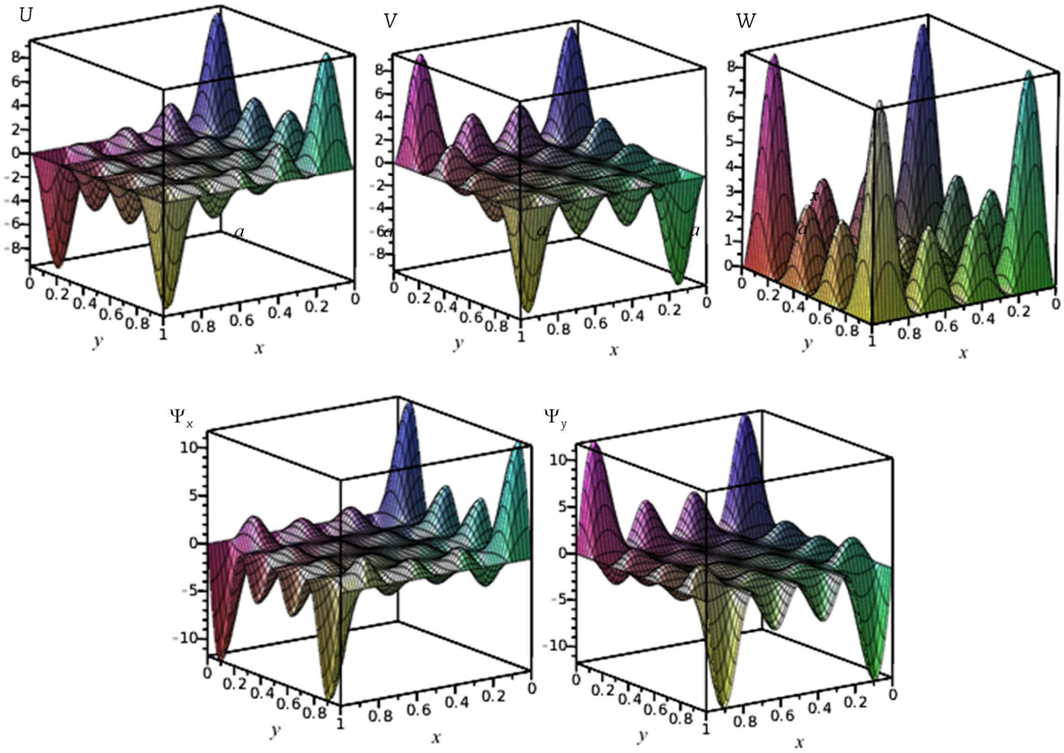

Fig. 3. Shape of approximation $\sum_{k=1}^{n}\sum_{l=1}^{n}X_1^kY_1^l, \sum_{k=1}^{n}\sum_{l=1}^{n}X_2^kY_2^l, \sum_{k=1}^{n}\sum_{l=1}^{n}X_3^kY_3^l, \sum_{k=1}^{n}\sum_{l=1}^{n}X_4^kY_4^l, \sum_{k=1}^{n}\sum_{l=1}^{n}X_5^kY_5^l$.

Consider simply support thin-walled shells (at $x = 0, x = a$: $U = V = W = M_x = \Psi_y = 0$; at $y = 0, y = b$: $U = V = W = M_y = \Psi_x = 0$). The following trigonometric functions can then be taken as approximating ones:

$$\begin{gathered} X_1^k = \sin\left(2k\pi\frac{x}{a}\right),\quad X_2^k = \sin\left((2k-1)\pi\frac{x}{a}\right),\quad X_3^k = \sin\left((2k-1)\pi\frac{x}{a}\right),\quad X_4^k = \cos\left((2k-1)\pi\frac{x}{a}\right),\quad X_5^k = \sin\left((2k-1)\pi\frac{x}{a}\right), \\ Y_1^l = \sin\left((2l-1)\pi\frac{y}{b}\right),\quad Y_2^l = \sin\left(2l\pi\frac{y}{b}\right),\quad Y_3^l = \sin\left((2l-1)\pi\frac{y}{b}\right),\quad Y_4^l = \sin\left((2l-1)\pi\frac{y}{b}\right),\quad Y_5^l = \cos\left((2l-1)\pi\frac{y}{b}\right). \end{gathered} \tag{5}$$

Figure 2 graphically shows all possible options for functions X^k. For Y^l, the function options are the same. The combination of the functions presented can replicate the symmetrical deformation shape of the structure. Figure 3 shows the sums of the products of functions $\sum_{k=1}^{n}\sum_{l=1}^{n}X_1^kY_1^l, \sum_{k=1}^{n}\sum_{l=1}^{n}X_2^kY_2^l, \sum_{k=1}^{n}\sum_{l=1}^{n}X_3^kY_3^l, \sum_{k=1}^{n}\sum_{l=1}^{n}X_4^kY_4^l, \sum_{k=1}^{n}\sum_{l=1}^{n}X_5^kY_5^l$, on the basis of which it can be concluded that the above boundary conditions are met.

The choice of trigonometric functions as the basis is due to the fact that they describe the process of deformation of the structure with the formation of dents rather well, and moreover, they satisfy the specified boundary conditions. In addition, for closed structures, they can satisfy the periodicity conditions, which is also important. The use of a large number of terms in (5) in the case of using trigonometric functions does not lead to a significant increase in the degrees of the variables, as in the case of polynomial approximation. In [31–34] one can finds the use of Legendre polynomials, in [34–37] – the use of Chebyshev polynomials as approximating functions. A comparison of trigonometric approximation and Legendre polynomials was carried out in [38].

By substituting Eq. (5) to Eq. (1), the functional E_s is transformed into the function E_{sf}. To find the minimum, it's need to find derivatives of the function E_{sf} with respect to all unknown numerical parameters and then equate those to zero. As a result, a system of nonlinear algebraic equations is obtained. To solve it, the best parameter continuation method, which makes it possible to reduce the solution of a nonlinear system to the solution of the initial problem for a system of ordinary differential equations, are used. The resulting initial problem can be solved using various methods, e.g. the Euler method.

In this case, the Maple analytical software package is the best option for software implementation, since fairly intensive symbolic computations are required.

This approach allows to explore the strength and buckling of shells, to bypass the singular points of curve "load – deflection" in order to obtain the values of upper and lower critical loads, find points of bifurcation, and investigate the supercritical behavior of shells. Buckling analysis of cylindrical and conical shell panels with an orthogonal grid of stiffeners was carried out by the author earlier in the work [39].

In this work, it will be analyzed the strength of the structure, which is based on the analysis of the strength criterion at each point of the structure with gradually increasing load values. Strength analysis is carried out according to the von Mises criterion, which in relation to the study of the strength of shell structures is written in the form:

$$\sigma_i \le \sigma_T,$$

where σ_i – stress intensity; σ_T – material yield strength. The stress intensity can be represented as

$$\sigma_i = \sqrt{\sigma_x^2 - \sigma_x\sigma_y + \sigma_y^2 + 3\left(\tau_{xy}^2 + \tau_{xz}^2 + \tau_{yz}^2\right)}. \tag{6}$$

Table 1. Options of panels under consideration

No.	h, m	a, m	b, rad	R_2, m
1	0.08	16	1	16
2	0.01	1.5	0.4	2.5

Table 2. Characteristics of the considered shells

No.	Parameter					
	S^0, m^2	V^0, m^3	a/h	d, m	$h^i = h^j$, m	$r_i = r_j$, m
1	256	20.48	200	1.96	0.24	0.16
2	1.5	0.015	150	0.05	0.03	0.02

Table 3. Characteristics of the considered shells depending on the number of stiffeners

No.		Characteristics depending on the number of stiffeners						
		2×2	4×4	6×6	8×8	12×12	16×16	20×20
1	x_r, m	8	4	2.67	2	1.33	1	0.8
	y_r, m	8	4	2.67	2	1.33	1	0.8
	S^R, m^2	10.14	20.07	29.80	39.32	57.75	75.37	92.16
	V^R, m^3	2.43	4.82	7.15	9.44	13.86	18.09	22.12
	S^R / S^0	0.040	0.078	0.116	0.154	0.226	0.294	0.360
	V^R / V^0	0.119	0.235	0.349	0.461	0.677	0.883	1.080
		2×2	4×4	6×6	8×8	12×12	16×16	20×20
2	x_r, m	0.75	0.375	0.25	0.188	0.125	0.09	0.075
	y_r, m	0.50	0.25	0.17	0.13	0.08	0.06	0.05
	S^R, m^2	0.098	0.194	0.286	0.374	0.542	0.698	0.840
	V^R, m^3	0.003	0.006	0.009	0.011	0.016	0.021	0.025
	S^R / S^0	0.066	0.129	0.190	0.250	0.362	0.465	0.560
	V^R / V^0	0.197	0.387	0.571	0.749	1.085	1.395	1.680

"Stress-strain" relationships for linearly elastic deformation of orthotropic materials in a plane stress state will have the form:

$$\sigma_x = \frac{E_1}{1-\mu_{12}\mu_{21}}\left[\varepsilon_x + \mu_{21}\varepsilon_y + z(\chi_1 + \mu_{21}\chi_2)\right],$$
$$\sigma_y = \frac{E_2}{1-\mu_{12}\mu_{21}}\left[\varepsilon_y + \mu_{12}\varepsilon_x + z(\chi_2 + \mu_{12}\chi_1)\right], \tag{7}$$
$$\tau_{xy} = G_{12}\left[\gamma_{xy} + 2z\chi_{12}\right],\ \ \tau_{xz} = G_{13}\gamma_{xz},\ \ \tau_{yz} = G_{23}\gamma_{yz}.$$

Despite the fact that further shell structures made of an isotropic material will be considered, the relations for the orthotropic case, as a more general one, are presents.

For consistency with other criteria [22] and convenience of further comparison, writes the von Mises criterion in the following form:

$$K_r = \frac{\sigma_i}{\sigma_T} \le 1. \tag{8}$$

3. Numerical Results

Calculations for three options of cylindrical panels (Table 1), based on the proposed model and algorithm, are performed. Geometric nonlinearity is taken into account. Type of support: pin support; loading: uniformly distributed static loading directed along the normal to the surface. Material: Steel S345 with $E_1 = E_2 = E = 2.1\cdot 10^5$ MPa, $\mu_{12} = \mu_{21} = \mu = 0.3$, $\sigma_T = 265 \div 345$ MPa. The parameters of S345 steel were taken in accordance with GOST 27772-2015 "Rolled steel for building steel structures. General specifications (with amendment No. 1)". It should be noted that the yield point will be different depending on the thickness of the rolled stock (from 265 MPa at a thickness of 0.08–0.16 m to 345 MPa at a thickness of 0.002–0.01 m). It will be take this into account when calculating the structures under consideration.

It's performed calculations at $N = 16$ summands under the approximation of the Ritz method.

The orthogonal grid of stiffeners is placed on the inside of the skin. The height and width of stiffeners are $h^i = h^j = 3h$, $r_i = r_j = 2h$, respectively. The number of stiffeners is equal in both directions, and for each new grid option, it is increased by 2 or 4. Stresses will be calculated with regard to the outer surface of the skin. Before presenting the calculation data, some characteristics of the considered shells depending on the number of stiffeners will be shown (Table 2, Table 3). Here S^0 – skin surface area; V^0 – skin volume; d – camber of arch; x_r – distance between stiffeners; S^R – stiffeners area; V^R – stiffeners volume.

Table 4. Maximum allowable loads for stiffened cylindrical panels

No.		N	Method	Maximum permissible load q_{pr}, MPa								Curve
				0×0	2×2	4×4	6×6	8×8	12×12	16×16	20×20	
1	$\sigma_T = 265$ MPa, $h = 0.08$ m	9	Refined model (Semenov)	0.2863	0.3938	0.3765	0.4411	0.4599	0.4962	0.5314	0.5658	–
		16		0.2693	0.2310	0.3450	0.4082	0.4230	0.4541	0.4828	0.5112	1
		9	Structural anisotropy method (Karpov)	0.2863	0.3500	0.3757	0.4409	0.4598	0.4961	0.5313	0.5658	–
		16		0.2693	0.3640	0.3899	0.4065	0.4229	0.4541	0.4828	0.5111	2
	$\sigma_T = 265$ MPa, $h = 0.01$ m	9	Refined model (Semenov)	0.5969	0.9658	1.1434	1.2289	1.2949	1.4066	1.5047	1.5412	–
		16		0.5943	0.9742	1.1575	1.2470	1.3146	1.4262	1.5218	1.6097	3
		9	Structural anisotropy method (Karpov)	0.5969	1.0377	1.1467	1.2289	1.2948	1.4065	1.5046	1.5412	–
		16		0.5943	1.0364	1.1581	1.2460	1.3145	1.4261	1.5218	1.6096	4
	$\sigma_T = 345$ MPa, $h = 0.01$ m	9	Refined model (Semenov)	0.6455	1.0942	1.4041	1.5398	1.6030	1.7541	1.8812	1.9464	–
		16		0.6196	1.1290	1.4044	1.5183	1.6172	1.7713	1.8979	2.0114	5
		9	Structural anisotropy method (Karpov)	0.6455	1.1995	1.4104	1.5403	1.6030	1.7541	1.8811	1.9463	–
		16		0.6196	1.1871	1.4100	1.5180	1.6172	1.7712	1.8978	2.0114	6
2	$\sigma_T = 265$ MPa, $h = 0.01$ m	9	Refined model (Semenov)	0.6608	0.7501	0.7991	0.8278	0.8592	0.9246	0.9653	1.0287	–
		16		0.6722	0.7891	0.8003	0.8509	0.8821	0.9246	0.9890	1.0529	7
		9	Structural anisotropy method (Karpov)	0.6608	0.7788	0.7991	0.8276	0.8591	0.9245	0.9653	1.0287	–
		16		0.6722	0.7845	0.8225	0.8506	0.8820	0.9245	0.9890	1.0529	8
	$\sigma_T = 345$ MPa, $h = 0.01$ m	9	Refined model (Semenov)	0.7008	0.9419	1.0078	1.0456	1.0866	1.1496	1.2328	1.3150	–
		16		0.7032	0.9944	1.0087	1.0675	1.1081	1.1711	1.2544	1.3368	9
		9	Structural anisotropy method (Karpov)	0.7008	0.9803	1.0077	1.0454	1.0864	1.1495	1.2327	1.3149	–
		16		0.7032	1.0046	1.0302	1.0671	1.1079	1.1711	1.2544	1.3368	10

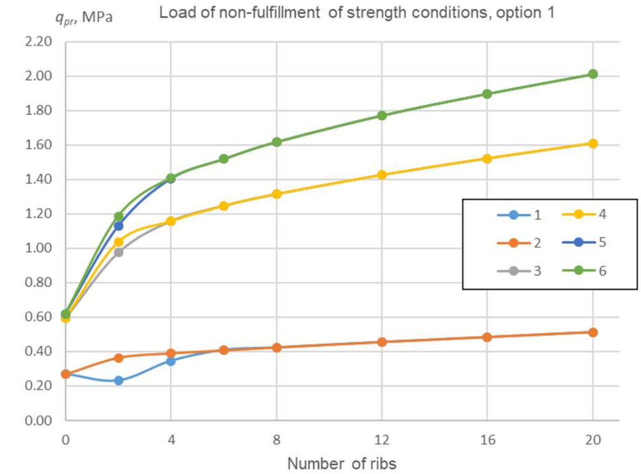

Fig. 4. The values of the maximum permissible load q_{pr} at different numbers of stiffeners (cylindrical panel 1, N = 16)

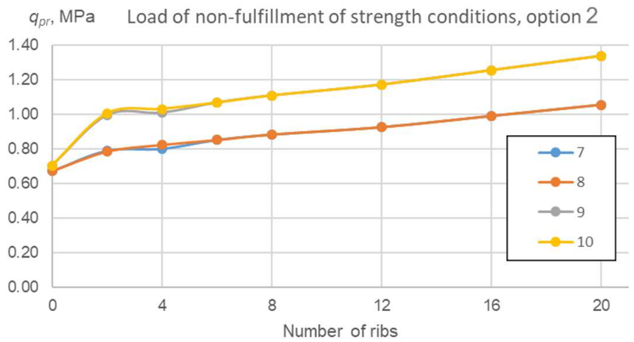

Fig. 5. The values of the maximum permissible load q_{pr} at different numbers of stiffeners (cylindrical panel 2, N = 16)

Table 4 shows the values of the maximum permissible strength loss loads for different stiffeners options, obtained using different methods of considering stiffeners and at different values of $N = n^2$. In Fig. 4, 5 results for $N = 16$ shown graphically (curve numbers are shown in Table 4). As can be seen from the data presented, the reinforcement of the structure with stiffeners increases its bearing capacity, this is especially noticeable when adding the first few stiffening elements. It is also seen that already with an orthogonal mesh of 6x6 edges, the values, obtained by the method of constructive anisotropy and the refined discrete method, converge.

Options in the Table 3 are highlighted in green for which further comparison will be made.

In Fig. 6 "load – deflection" dependence for a cylindrical panel (option 1, $N = 16$) with orthogonal grids of stiffeners 0×0, 8×8 are shown. The red curve W_c in the Fig. 6 depicts the deflection in the center of a structure $(x = a/2, y = b/2)$, and the blue curve W_4 the deflection in the quadrant of a structure $(x = a/4, y = b/4)$.

The buckling load is detected as follows: the load/deflection diagram is analyzed, where a small change in the load corresponds to a significant change in the deflection (Lyapunov criterion), and snap-through buckling (transition to a new equilibrium state) occurs. In software, the moment when the determinant of the Jacobi matrix J becomes zero also corresponds to the critical load. It should be noted that condition $detJ = 0$ may also correspond to lower critical loads and bifurcation points.

For considered cylindrical panel 1, critical buckling load are 0.6897 MPa (for orthogonal grids of stiffeners 0×0) and 3.1806 MPa (orthogonal grids of stiffeners 8×8).

In accordance with the data obtained, Figs. 7 and 8 show the fields of criterion (8) at loads for which the strength condition ceases to be met. Areas of the structure for which the criterion ceases to be met correspond to the parts where the criterion field exceeds the value $K_r = 1$. The criterion field has a complex shape, for its better interpretation in Fig. 7, 8 added transparency.

In Fig. 9 the extension of areas of non-fulfillment of the strength conditions (8) for the cylindrical panel 1 is shown with an increase in the value of the load already after the initial destruction of the material according to the von Mises criterion.

As can be seen from the presented data, areas of non-fulfillment of strength conditions appear near the edge of the circumferential coordinate, then develop along it, uniting, and then begin to gradually spread to the center of the structure. In the presence of stiffeners, this process develops under higher loads than for unstiffened structures.

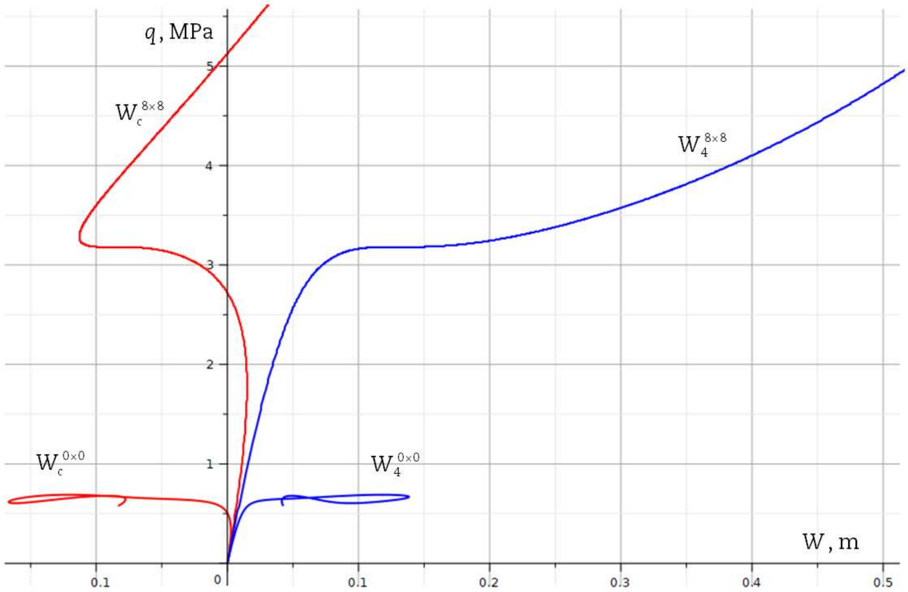

Fig. 6. Load – deflection dependence for a cylindrical panel (option 1, N = 16) with orthogonal grids of stiffeners 0×0, 8×8.

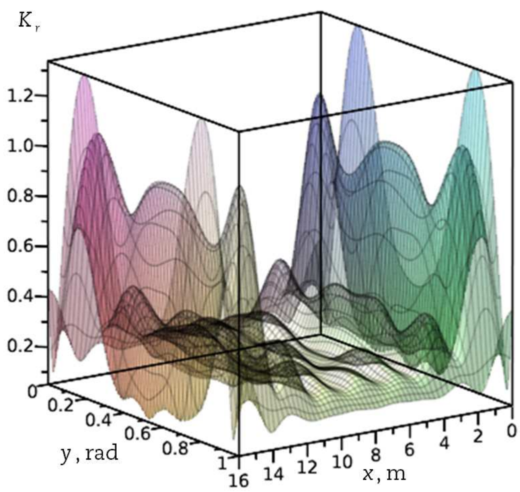

Fig. 7. The von Mises criterion field (8) for the option 1 panel (N = 16, 0×0 grid of stiffeners) under load 0.2692 MPa

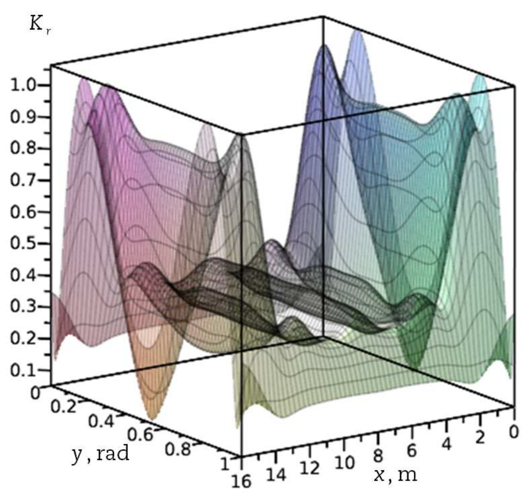

Fig. 8. The von Mises criterion field (8) for the option 1 panel (N = 16, 8×8 grid of stiffeners) under load 0.4229 MPa

4. Conclusion

A study of the strength of thin-walled cylindrical panels, reinforced with stiffeners, was carried out. The analysis of approaches to the introduction of stiffeners has been carried out, which has shown that the proposed improved version of taking into account the stiffness characteristics gives a result close to the method of constructive anisotropy. In addition, the convergence of the constructive anisotropy method is shown with an increase in the number of reinforcing elements. Using it instead of discrete approaches to the introduction of edges can significantly reduce the calculation time. Shown are three-dimensional graphs of the strength criterion at a specific load value. The analysis of the extension of areas of non-fulfillment of strength conditions according to the Mises criterion for the structures under consideration is carried out. Their size is shown in the presence and absence of stiffeners for the same load values. The proposed format for presenting data on areas of non-fulfillment of strength conditions and graph of strength criterion is new and makes it possible to visually assess the state of the structure.

Author Contributions

The manuscript was written through the contribution of one author. Author discussed the results, reviewed, and approved the final version of the manuscript.

Acknowledgments

Not Applicable.

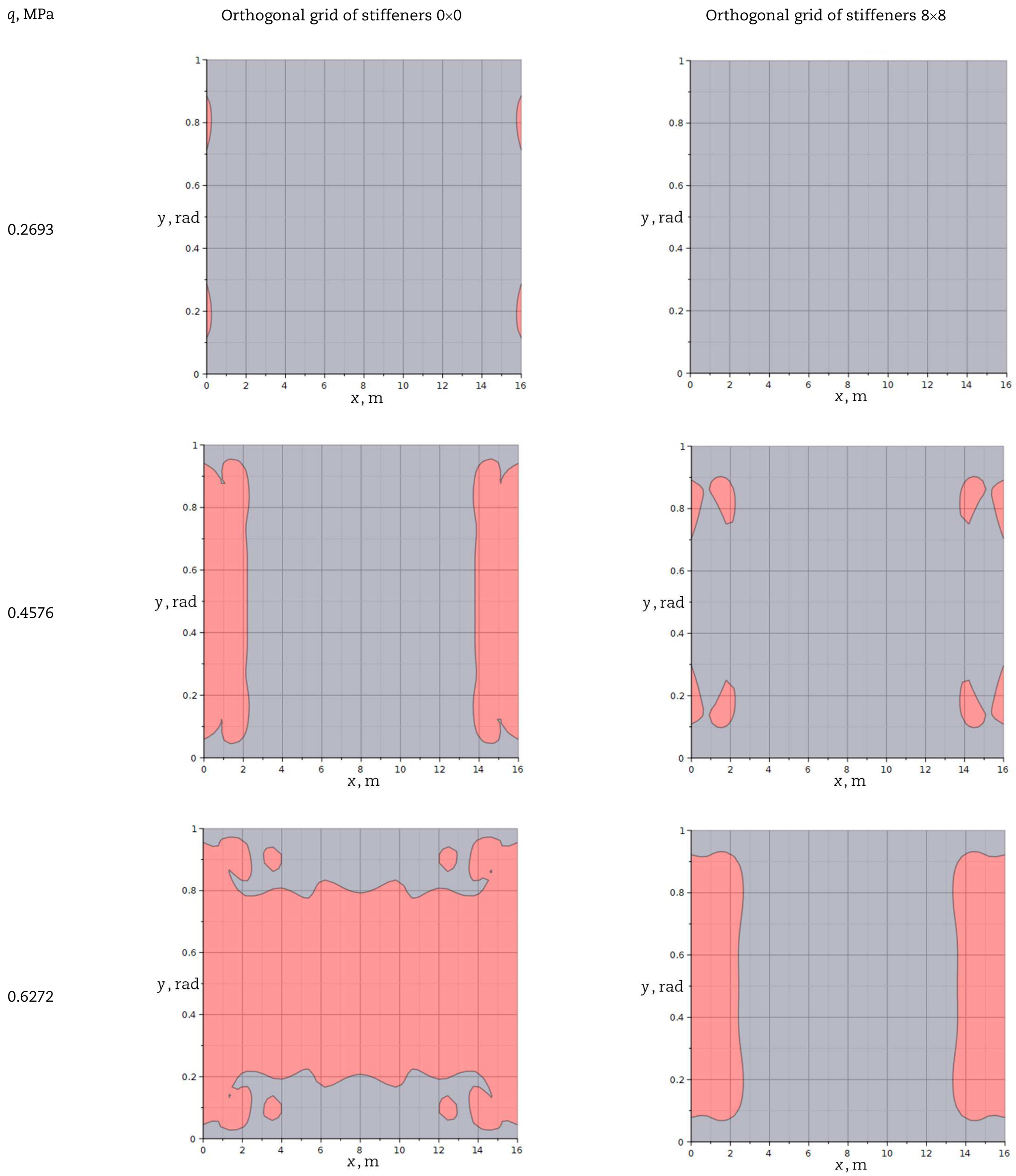

Fig. 9. Comparison of areas of non-fulfillment of strength conditions (when the value of the criterion $K_r \geq 1$) for cylindrical panel 1 with stiffeners grid 0×0, 8×8 and with increasing load values

Conflict of Interest

The author declared no potential conflicts of interest with respect to the research, authorship, and publication of this article.

Funding

The author received no financial support for the research, authorship, and publication of this article.

Data Availability Statements

Not Applicable.

Nomenclature

A, B	Lame parameters describing the shell geometry;	q, P_x, P_y	Load components;
E_1, E_2	Elastic moduli;	q_{cr}	Critical buckling load;
E_s	Functional of full potential deformation energy of the shell structure;	q_{pr}	Maximum permissible load (strength);
E_s^0	Functional of full potential deformation energy of the skin;	Q_x, Q_y	Transverse forces in the planes *xOz* and *yOz*;
E_p^R	Potential deformation energy of the stiffeners;	U, V, W	Displacement functions;
$f(z)$	Function describing the distribution of stresses τ_{xz} and τ_{yz} through the shell thickness;	W_c	Deflection in the center of a structure;
G_{12}, G_{13}, G_{23}	Shear modules;	W_4	Deflection in the quadrant of a structure;
k_x, k_y	Main curvatures of the shell along the *x* and *y* axes;	γ_{xy}	Shear deformation in the *xOy* plane;
K_r	Yield strength criterion;	χ_1, χ_2, χ_{12}	Functions of curvature and torsional change;
M_x, M_y, M_{xy}, M_{yx}	Moments, occurring in the structure;	Ψ_x, Ψ_y	Functions of the normal rotation angles in the *xOz* and *yOz* planes, respectively;
M_x^0, M_y^0, M_{xy}^0, M_{yx}^0	Moments, occurring in the skin;	$\varepsilon_x, \varepsilon_y$	Deformations of elongation along the x, y coordinates of the middle surface;
M_x^R, M_y^R, M_{xy}^R, M_{yx}^R	Forces and moments, occurring in the stiffeners;	μ_{12}, μ_{21}	Poisson's ratios;
N_x, N_y, N_{xy}, N_{yx}	Forces, occurring in the structure;	σ_x, σ_y	The normal stresses in the directions of axes x, y;
N_x^0, N_y^0, N_{xy}^0, N_{yx}^0	Forces, occurring in the skin;	$\tau_{xy}, \tau_{xz}, \tau_{yz}$	Shear stresses in the plane xOy, xOz and yOz;
N_x^R, N_y^R, N_{xy}^R, N_{yx}^R	Forces and moments, occurring in the stiffeners;	σ_i	Stress intensity;
N	Number of terms in the expansion of Ritz method;	σ_T	Material yield strength.

References

[1] Bischoff, M., Bletzinger, K.-U., Wall, W.A., Ramm, E., Models and Finite Elements for Thin-Walled Structures, *In: Encyclopedia of Computational Mechanics*, ed. Stein E., de Borst R., Hughes T.J.R. Chichester, UK: John Wiley & Sons, Ltd, 2004, 59–137. DOI: 10.1002/0470091355.ecm026.
[2] Godoy, L.A., *Thin-Walled Structures with Structural Imperfections*, Elsevier, 1996. DOI: 10.1016/B978-0-08-042266-4.X5000-3.
[3] Mamalis, A.G., Manolakos, D.E., Demosthenous, G.A., Ioannidis M.B., *Crashworthiness of composite thin-walled structural components*, Boca Raton; London; New York: CRC Press, Taylor & Francis Group, 2019.
[4] Fragassa, C., Minak, G., Pavlovic, A., Measuring deformations in the telescopic boom under static and dynamic load conditions, *Facta Universitatis-Series Mechanical Engineering*, 18(2), 2020, 315–328. DOI: 10.22190/FUME181201001F.
[5] Jaunky, N., Knight, N.F., Ambur, D.R., Formulation of an improved smeared stiffener theory for buckling analysis of grid-stiffened composite panels, *Composites Part B: Engineering*, 27(5), 1996, 519–526. DOI: 10.1016/1359-8368(96)00032-7.
[6] Kidane, S., Li, G., Helms, J., Pang, S.-S., Woldesenbet, E., Buckling load analysis of grid stiffened composite cylinders, *Composites Part B: Engineering*, 34(1), 2003, 1–9. DOI: 10.1016/S1359-8368(02)00074-4.
[7] Wang, J.T.-S., Hsu, T.-M., Discrete analysis of stiffened composite cylindrical shells, *AIAA Journal*, 23(11), 1985, 1753–1761. DOI: 10.2514/3.9162.
[8] Meish, V.F., Meish, Yu.A., Pavlyuk, A.V., Dynamics of a Three-Layer Elliptic Cylindrical Shell Reinforced with Discrete Rings, *International Applied Mechanics*, 54(2), 2018, 172–179. DOI: 10.1007/s10778-018-0869-z.
[9] Qu, Y., Wu, S., Chen, Y., Hua, H., Vibration analysis of ring-stiffened conical-cylindrical-spherical shells based on a modified variational approach, *International Journal of Mechanical Sciences*, 69, 2013, 72–84. DOI: 10.1016/j.ijmecsci.2013.01.026.
[10] Sadeghifar, M., Bagheri, M., Jafari, A.A., Buckling analysis of stringer-stiffened laminated cylindrical shells with nonuniform eccentricity, *Archive of Applied Mechanics*, 81(7), 2011, 875–886. DOI: 10.1007/s00419-010-0457-0.
[11] Talebitooti, M., Ghayour, M., Ziaei-Rad, S., Talebitooti, R., Free vibrations of rotating composite conical shells with stringer and ring stiffeners, *Archive of Applied Mechanics*, 80(3), 2010, 201–215. DOI: 10.1007/s00419-009-0311-4.
[12] Troitsky, M.S., *Stiffened plates: bending, stability, and vibrations*, Elsevier Scientific Pub. Co., Amsterdam; New York, 1976.
[13] Reddy, A.D., Valisetty, R., Rehfield, L.W., Continuous filament wound composite concepts for aircraft fuselage structures, *Journal of Aircraft*, 22(3), 1985, 249–255. DOI: 10.2514/3.45115.
[14] Dung, D.V., Chan, D.Q., Analytical investigation on mechanical buckling of FGM truncated conical shells reinforced by orthogonal stiffeners based on FSDT, *Composite Structures*, 159, 2017, 827–841. DOI: 10.1016/j.compstruct.2016.10.006.
[15] Tu, T.M., Loi, N.V., Vibration Analysis of Rotating Functionally Graded Cylindrical Shells with Orthogonal Stiffeners, *Latin American Journal of Solids and Structures*, 13(15), 2016, 2952–2969. DOI: 10.1590/1679-78252934.
[16] Lanzo, A.D., Garcea, G., Koiter's analysis of thin-walled structures by a finite element approach, *International Journal for Numerical Methods in Engineering*, 39(17), 1996, 3007–3031. DOI: 10.1002/(SICI)1097-0207(19960915)39:17<3007::AID-NME991>3.0.CO;2-S.
[17] Pinto, V.T., Oliveira Rocha, L.A., Fragassa, C., Domingues dos Santos, E., Isoldi, L.A., Multiobjective Geometric Analysis of Stiffened Plates under Bending through Constructal Design Method, *Journal of Applied and Computational Mechanics*, 6(SI), 2020, 1438–1449. DOI: 10.22055/jacm.2020.35248.2608.
[18] Bai, X., Xu, W., Ren, H., Li, J., Analysis of the influence of stiffness reduction on the load carrying capacity of ring-stiffened cylindrical shell, *Ocean Engineering*, 135, 2017, 52–62. DOI: 10.1016/j.oceaneng.2017.02.034.
[19] Chen, B., Liu, G., Kang, J., Li, Y., Design optimization of stiffened storage tank for spacecraft, *Structural and Multidisciplinary Optimization*, 36(1), 2008, 83–92. DOI: 10.1007/s00158-007-0174-7.
[20] Lene, F., Duvaut, G., Olivier-Mailhe, M., Ben Chaabane, S., Grihon, S., An advanced methodology for optimum design of a composite stiffened cylinder, *Composite Structures*, 91(4), 2009, 392–397. DOI: 10.1016/j.compstruct.2009.04.005.
[21] Reza Ghasemi, A., Tabatabaeian, A., Hadi Hajmohammad, M., Tornabene, F., Multi-Step Buckling Optimization Analysis of Stiffened and Unstiffened Polymer Matrix Composite Shells: A New Experimentally Validated Method, *Composite Structures*, 273, 2021, 114280. DOI: 10.1016/j.compstruct.2021.114280.
[22] Hao, P., Wang, B., Tian, K., Liu, H., Wang, Y., Niu, F., Zeng, D., Simultaneous buckling design of stiffened shells with multiple cutouts, *Engineering Optimization*, 49(7), 2017, 1116–1132. DOI: 10.1080/0305215X.2016.1235328.
[23] Wang, J., Li, Z.L., Yu, W., Structural similitude for the geometric nonlinear buckling of stiffened orthotropic shallow spherical shells by energy approach, *Thin-Walled Structures*, 138, 2019, 430–457. DOI: 10.1016/j.tws.2018.02.006.
[24] Cho, S.-R., Muttaqie, T., Do, Q.T., Park, S.H., Kim, S.M., So, H.Y., Sohn, J.M., Experimental study on ultimate strength of steel-welded ring-stiffened conical shell under external hydrostatic pressure, *Marine Structures*, 67, 2019, 102634. DOI: 10.1016/j.marstruc.2019.102634.
[25] Duarte, A.P.C., Díaz Sáez, A., Silvestre, N., Comparative study between XFEM and Hashin damage criterion applied to failure of composites, *Thin-Walled Structures*, 115, 2017, 277–288. DOI: 10.1016/j.tws.2017.02.020.

[26] Brauns, J., Skadins, U., Semi-analytical postbuckling strength analysis of anisotropic shell structures, *IOP Conference Series: Materials Science and Engineering*, 251, 2017, 012096. DOI: 10.1088/1757-899X/251/1/012096.
[27] Abrosimov, N.A., Novoseltseva, N.A., Computer Modeling of the Dynamic Strength of Metal-Plastic Cylindrical Shells Under Explosive Loading, *Mechanics of Composite Materials*, 53, 2017, 139–148. DOI: 10.1007/s11029-017-9648-x.
[28] Semenov, A.A., Analysis of the strength of shell structures, made from modern materials, according to various strength criteria, *Diagnostics, Resource and Mechanics of Materials and Structures*, 2018, 16–33. DOI: 10.17804/2410-9908.2018.1.016-033.
[29] Pavlovic, A., Sintoni, D., Fragassa, C., Minak, G., Multi-Objective Design Optimization of the Reinforced Composite Roof in a Solar Vehicle, *Applied Sciences*, 10(8), 2020, 2665. DOI: 10.3390/app10082665.
[30] Karpov, V.V., Semenov, A.A., Refined model of stiffened shells, *International Journal of Solids and Structures*, 199, 2020, 43–56. DOI: 10.1016/j.ijsolstr.2020.03.019.
[31] Li, G., de Miguel, A.G., Pagani, A., Zappino, E., Carrera, E., Finite beam elements based on Legendre polynomial expansions and node-dependent kinematics for the global-local analysis of composite structures, *European Journal of Mechanics – A/Solids*, 74, 2019, 112–123. DOI: 10.1016/j.euromechsol.2018.11.006.
[32] Yshii, L.N., Santana, R.C., Monteiro, F.A.C., Lucena Neto, E., Buckling of Cylindrical Panels by a Ritz Scheme, *Proceedings of the XXXVIII Iberian Latin-American Congress on Computational Methods in Engineering*, Brazil, 2017. DOI: 10.20906/CPS/CILAMCE2017-0613.
[33] Feng, K., Xu, J., Buckling Analysis of Composite Cylindrical Shell Panels by Using Legendre Polynomials Hierarchical Finite-Strip Method, *Journal of Engineering Mechanics*, 143(4), 2017, 04016121. DOI: 10.1061/(ASCE)EM.1943-7889.0001181.
[34] Qu, Y., Long, X., Wu, S., Meng, G., A unified formulation for vibration analysis of composite laminated shells of revolution including shear deformation and rotary inertia, *Composite Structures*, 98, 2013, 169–191. DOI: 10.1016/j.compstruct.2012.11.001.
[35] Monge, J.C., Mantari, J.L., A quasi-exact solution for the analysis of smart multilayered simply supported shallow shell panels, *Composite Structures*, 265, 2021, 113710. DOI: 10.1016/j.compstruct.2021.113710.
[36] Qu, Y., Chen, Y., Long, X., Hua, H., Meng, G., A modified variational approach for vibration analysis of ring-stiffened conical-cylindrical shell combinations, *European Journal of Mechanics – A/Solids*, 37, 2013, 200–215. DOI: 10.1016/j.euromechsol.2012.06.006.
[37] Kurylov, Ye., Amabili, M., Nonlinear vibrations of clamped-free circular cylindrical shells, *Journal of Sound and Vibration*, 330(22), 2011, 5363–5381. DOI: 10.1016/j.jsv.2011.05.037.
[38] Bakusov, P.A., Semenov, A.A., Stability of Toroidal Shell Segments at Variation of a Deflection Angle, *PNRPU Mechanics Bulletin*, 3, 2017, 17–36. DOI: 10.15593/perm.mech/2017.3.02. (in Russian)
[39] Semenov, A., Buckling of Shell Panels Made of Fiberglass and Reinforced with an Orthogonal Grid of Stiffeners, *Journal of Applied and Computational Mechanics*, 7(3), 2021, 1856–1861. DOI: 10.22055/jacm.2021.37768.3078.

ORCID iD

Alexey Semenov https://orcid.org/0000-0001-9490-7364

How to cite this article: Semenov A. Strength of Steel Shell Cylindrical Panels Reinforced with an Orthogonal Grid of Stiffeners, *J. Appl. Comput. Mech.*, 8(2), 2022, 723–732. https://doi.org/10.22055/JACM.2022.38968.3317